Interplay between the exchange and Coulomb interactions in a ferromagnetic semiconductor quantum dot

N. Lebedeva, H. Holmberg, and P. Kuivalainen
Department of Micro and Nanosciences, TKK Helsinki University of Technology, P.O. Box 3500, FI-02015 TKK, Finland
(Received 25 February 2008; revised manuscript received 30 April 2008; published 9 June 2008)

We study the effects of the strong *sp-d* exchange interaction, ferromagnetic ordering, and large spin fluctuations on quantum transport in a ferromagnetic semiconductor quantum dot (FSQD) coupled to nonmagnetic current leads. The retarded Green's function for a FSQD in the Coulomb blockade regime is calculated using a simple equation of motion technique. The dot level broadening due to *sp-d* exchange interaction between the charge carrier spins and the localized magnetic moments of the magnetic atoms is considered within a self-consistent Born approximation. We also calculate the giant Zeeman splitting of the dot levels, the conductance, and the spin accumulation on the dot. The model predicts a large dot level broadening due to spin-disorder scattering, especially at temperatures close to the ferromagnetic ordering temperature. Our main finding is that in a small FSQD with a large intradot Coulomb repulsion the unusual temperature and magnetic field dependences of the level broadening give rise to a conductance behavior, which is similar to the Kondo resonance in QDs, even when the higher order correlations in the current leads are neglected.

DOI: 10.1103/PhysRevB.77.245308 PACS number(s): 73.23.Hk, 75.50.Pp, 73.21.La, 72.10.−d

I. INTRODUCTION

Spin physics has become one of the most studied branches of solid-state physics. Also a lot of new ideas as well as device realizations in the context of spin electronics (spintronics) have been reported in recent years.[1–4] One of the most challenging applications of spintronics is the quantum computer, which would represent a breakthrough in information processing.[1,5] Due to the reduced dimensionality and long-lived spin states quantum dots (QDs) have been proposed as building blocks for the implementation of quantum bits (qubits) for quantum computation.[6,7] Recent experiments[8–13] show that electrons in QDs have a long spin relaxation time [up to 20 ms (Ref. 10)] and it is now possible to coherently control the electron states and spin in QDs with a precision up to a single electron. Electronic transport studies through QDs provide a valuable tool for investigating various novel physical phenomena, such as the Coulomb blockade (CB),[14,15] the spin blockade,[16] and the tunneling magnetoresistance.[17]

Much recent effort in semiconductor spintronics has been devoted to the development of ferromagnetic semiconductors, which are created by doping conventional semiconductors, such as GaAs, with magnetic ions to concentrations of a few percent.[18–20] In these materials, the strong *sp-d* exchange interaction between charge carriers and the magnetic ions results in, e.g., a resistivity peak at the Curie temperature T_C due to spin-disorder scattering and a giant Zeeman splitting of the electronic states. Interesting novel possibilities arise when QD structures are combined with magnetic semiconductor materials. The diluted magnetic QDs have been grown using material systems based on II-VI semiconductors, such as CdMnTe/ZnTe (Refs. 21 and 22) or CdSe/ZnMnSe.[23] In this way magnetic QDs with a few or even single Mn atoms in the dot can be fabricated.[24,25] An advantage of the magnetic QDs is that they offer a way to study the interaction between a controlled number of injected carriers and the magnetic ions. A versatile control of the number of carriers, spin, and the quantum confinement could lead to improved transport, optical, and magnetic properties.[26] Recently, the first high T_C ferromagnetic semiconductor quantum dots (FSQDs) have been grown using Co-doped CdSe (Ref. 27) and ZnO,[28] and Mn-doped InAs.[29] Also the first single electron transistor (SET) made of ferromagnetic Mn-doped GaAs has been reported, which, in addition to CB oscillations, showed a large anisotropic magnetoresistance effect at low temperatures.[30] A new possibility in FSQDs would be the separate control of the Coulomb and the *sp-d* exchange interactions simply by adjusting the size of the dots.

In QDs new states of many-body character are created at the Fermi level at low temperatures by the Kondo effect, which has inspired both theory[31–33] and experiment.[34–37] The main signatures of the Kondo effect are a zero-bias conductance resonance, its specific temperature dependence, and a splitting of the resonance in a magnetic field. The origin of the Kondo resonance is related to higher order tunneling of correlated spin pairs between the quantum dot and the leads at temperatures below the Kondo temperature. In this paper, we study the effect of level broadening due to the strong *sp-d* exchange interaction on quantum transport in a FSQD. We predict that in a small FSQD with large intradot Coulomb interaction all the specific features of the Kondo resonance may appear even when the higher order correlations in the leads are neglected completely. Previously transport across a QD with a single magnetic ion[38,39] or through a magnetic semiconductor QD embedded in a tunneling barrier[40] have been studied theoretically. Also spin-dependent tunneling in QDs with ferromagnetic leads and in ferromagnetic SETs has been discussed thoroughly.[41–47] In spite of all this activity, to the best of our knowledge, no work has been done on spin-dependent transport in a FSQD. Especially, the effect of the large spin fluctuations and the ferromagnetic ordering on the dot level broadening in a FSQD have not been considered previously. In nonmagnetic QDs, intradot spin-flip scattering due to spin-orbit interaction has been studied by several

groups.[48–51] Also electron spin relaxation induced by phonon-mediated *sp*-exchange interaction in a II-VI magnetic semiconductor QD has been investigated.[52] Here we study quantum transport in a FSQD by calculating the temperature and magnetic field dependences of the conductance in the Coulomb blockade regime. We present a detailed model for a FSQD including a large on-site Coulomb repulsion and the strong *sp-d* exchange interaction between the charge carriers and the magnetic ions. By using an equation of motion technique, we calculate the retarded Green's function for a FSQD, and the level broadening due to the spin-disorder scattering is calculated within the self-consistent Born approximation.

The paper is organized as follows. In Sec. II we describe the model Hamiltonian for a FSQD. In Sec. III we present formulation based on Zubarev's double-time-Green's functions.[53] We also give explicit formulas for the level broadening. In Sec. IV we present numerical results for the level broadening, conductance, and spin accumulation in a FSQD based on Sec. III. Finally, in Sec. V we give some final remarks.

II. MODEL HAMILTONIAN FOR THE FSQD

We study the system of a ferromagnetic semiconductor quantum dot coupled to two nonmagnetic leads by tunneling processes through thin barriers on the left (L) and right (R) sides of the dot, as shown schematically in Fig. 1. An additional electrode provides the gate voltage V_g on the dot, which can change the position of the energy levels of the dot with respect to the Fermi energy E_F. We assume a disklike quantum dot with a radius R_0 and height z_0. The ferromagnetic subsystem consists of the localized magnetic electrons such as the five $3d$ electrons/atom on the Mn ion.

The spin operator for the total spin on a magnetic atom at a lattice site $\vec{R}$ is denoted by $\vec{S}_{\vec{R}}$. Then a Heisenberg-type Hamiltonian for the ferromagnetic subsystem inside the FSQD is given by

$$H_M = -\sum_{\vec{R},\vec{R}'} I(\vec{R},\vec{R}')\vec{S}_{\vec{R}} \cdot \vec{S}_{\vec{R}'} - g_L \mu_B B \sum_{\vec{R}} S^z_{\vec{R}}, \tag{1}$$

where $I(\vec{R},\vec{R}')$ is the ferromagnetic coupling constant between the localized spins, and the last term gives the ordinary Zeeman energy when an external magnetic field $\vec{B}$ has been applied in the z direction, i.e., in the growth direction of the dot. The average spin polarization of the ferromagnetic atoms can be calculated, e.g., in the mean-field approximation (see below).

When considering the charge carrier system on the QD, we assume a quantum well-type potential confinement in the z direction with a large band offset and an in-plane parabolic confining potential in the x and y directions. Then the solutions of the Schrödinger equation $H^0_{\mathrm{QD}}\psi_{nm\sigma} = E^0_{nm\sigma}\psi_{nm\sigma}$ are the well-known Fock–Darwin states[54] $\psi_{nm\sigma}(\vec{r}) = \psi_{nm}(\vec{r})\alpha(\sigma)$ with the eigenvalues $E^0_{nm\sigma}$. Here $\alpha(\sigma)$ is the eigenfunction of the Pauli spin operator $\vec{\sigma}$, and the indices n and m refer to the radial and angular quantum numbers, respectively. The calculation of the Green's functions below requires the presentation of the Hamiltonian in the second quantization formalism. Therefore, by using the wave functions $\psi_{nm\sigma}(\vec{r})$, we can define the following field operators for the charge carriers on the QD:

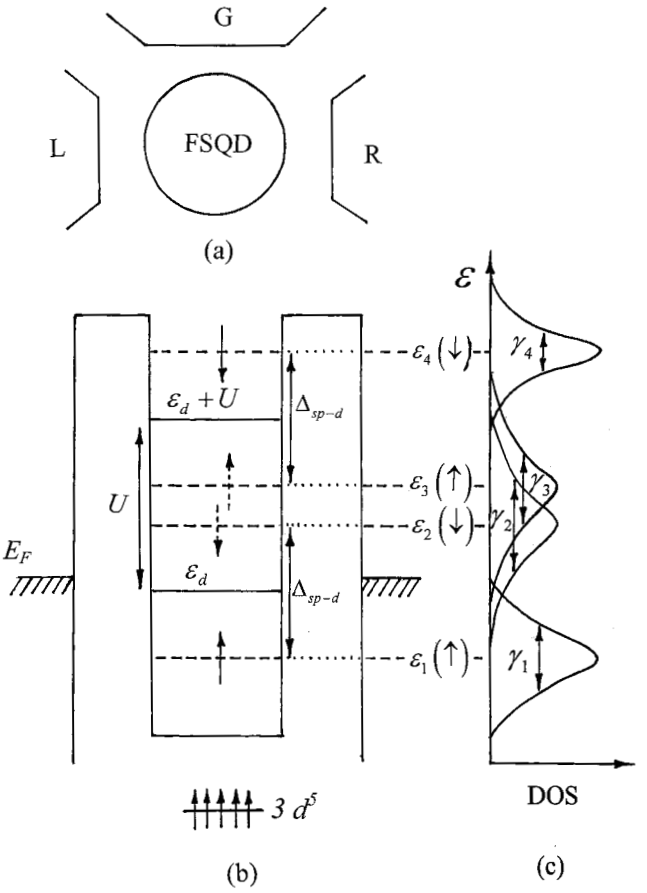

FIG. 1. Schematic drawing of the structure, energy diagram, and density of states (DOS) of the FSQD including two-spin degenerate dot levels ε^0_d and $\varepsilon^0_d + U$ with the on-site Coulomb repulsion U. The two levels are split to four levels $\varepsilon_1(\uparrow) = \varepsilon^0_d - \Delta_{sp\text{-}d}/2$, $\varepsilon_2(\downarrow) = \varepsilon^0_d + \Delta_{sp\text{-}d}/2$, $\varepsilon_3(\uparrow) = \varepsilon^0_d - \Delta_{sp\text{-}d}/2 + U$, and $\varepsilon_4(\downarrow) = \varepsilon^0_d + \Delta_{sp\text{-}d}/2 + U$ due to the giant Zeeman splitting $\Delta_{sp\text{-}d}$ [see Eq. (10)] caused by the *sp-d* exchange interaction (9) between the charge carriers and the magnetic $3d$ electrons of the magnetic ions on the dot. The exchange interaction also broadens the levels, as shown schematically in the DOS. Here γ_i's are the imaginary parts of the self-energy (27) related to the *sp-d* interaction.

$$\hat{\Psi}(\vec{r}) = \sum_{nm\sigma} \psi_{nm\sigma}(\vec{r}) d_{nm\sigma}, \tag{2}$$

$$\Psi^\dagger(\vec{r}) = \sum_{nm\sigma} \psi^*_{nm\sigma}(\vec{r}) d^\dagger_{nm\sigma}, \tag{3}$$

where the operator $d^\dagger_{nm\sigma}(d_{nm\sigma})$ creates (destroys) a charge carrier with spin σ on the level $|nm\sigma\rangle$. By using Eqs. (2) and (3), we can express the noninteracting dot Hamiltonian as

$$\hat{H}^0_{\mathrm{QD}} = \int d^3\vec{r}\Psi^\dagger(\vec{r}) H^0_{\mathrm{QD}}(\vec{r})\Psi(\vec{r}) = \sum_{nm\sigma} E^0_{nm\sigma} d^\dagger_{nm\sigma} d_{nm\sigma}. \tag{4}$$

Next we can add the perturbations to the Hamiltonian (4). The magnetic and electronic subsystems in the FSQD are coupled by the *sp-d* exchange interaction, which can be divided into a mean-field part and a fluctuating part,

$$\begin{aligned} H_{sp\text{-}d} &= H^0_{sp\text{-}d} + V_{sp\text{-}d} \\ &= -\sum_{\vec{R}} J_{sp\text{-}d}(\vec{r}-\vec{R})\vec{s}\cdot\langle\vec{S}_{\vec{R}}\rangle \\ &\quad -\sum_{\vec{R}} J_{sp\text{-}d}(\vec{r}-\vec{R})\vec{s}\cdot(S_{\vec{R}}-\langle\vec{S}_{\vec{R}}\rangle), \end{aligned} \tag{5}$$

where $J_{sp\text{-}d}(\vec{r}-\vec{R})$ is the *sp-d* exchange interaction potential, which is assumed to be of the contact-potential type, and it is given by

$$J(\vec{r}-\vec{R}) = J_{sp\text{-}d}\Omega\,\delta(\vec{r}-\vec{R})\,\theta(R_0-\rho). \tag{6}$$

Here $J_{sp\text{-}d}$ is the *sp-d* exchange interaction parameter, Ω is the volume of the unit cell, $\rho=(x,y)$ and the Heaviside unit step function θ restrict the potential (6) to the FSQD. The mean-field part $H^0_{sp\text{-}d}$ causes the giant Zeeman splitting of the electronic states in the FSQD in the cases where the average spin polarization $\langle\vec{S}_{\vec{R}}\rangle$ is nonvanishing. On the other hand, the fluctuating part $V_{sp\text{-}d}$ gives rise to spin-disorder scattering of the charge carriers, which in the ferromagnetic semiconductors may be the dominant scattering mechanism at temperatures close to T_C.[55] With the field operators (2) and (3) and the exchange potential (6), we can express the exchange interaction Hamiltonian (5) in the second quantization form,

$$\hat{H}_{sp\text{-}d} = \int d^3\vec{r}\Psi^\dagger(\vec{r})H_{sp\text{-}d}\Psi(\vec{r}) = \hat{H}^0_{sp\text{-}d} + \hat{V}_{sp\text{-}d}, \tag{7}$$

with

$$\hat{H}^0_{sp\text{-}d} = -\frac{1}{2}\Delta^{nm}_{sp\text{-}d}\sum_{nm}(d^\dagger_{nm\uparrow}d_{nm\uparrow} - d^\dagger_{nm\downarrow}d_{nm\downarrow}), \tag{8}$$

and

$$\begin{aligned} \hat{V}_{sp\text{-}d} = -\left(\frac{J_{p\text{-}d}\Omega}{2}\right) \sum_{\substack{nm\sigma \\ n'm'\sigma' \\ \vec{R}\in \mathrm{FSQD}}} & \psi^*_{nm}(\vec{R})\psi_{n'm'}(\vec{R})[S^+_{\vec{R}}d^\dagger_{nm\downarrow}d_{nm\uparrow} \\ & + S^-_{\vec{R}}d^\dagger_{nm\uparrow}d_{nm\downarrow} + (S^z_{\vec{R}} - \langle S^z_{\vec{R}}\rangle)(d^\dagger_{nm\uparrow}d_{nm\uparrow} - d^\dagger_{nm\downarrow}d_{nm\downarrow})], \end{aligned} \tag{9}$$

where $\Delta^{nm}_{sp\text{-}d}$ is the temperature and magnetic field dependent spin-splitting parameter, which is given by

$$\Delta^{nm}_{sp\text{-}d}(T,B) = xJ_{sp\text{-}d}\langle S^z(T,B)\rangle\Omega F_{nm}, \tag{10}$$

with

$$F_{nm} = \sum_{\vec{R}\in \mathrm{FSQD}} |\psi_{nm}(\vec{R})|^2. \tag{11}$$

Here x is the mole fraction of the magnetic atoms, $x\langle S^z\rangle = \sum_{\vec{R}}\langle S^z_{\vec{R}}\rangle/N$, and N is the number of unit cells. The weight factor F_{nm} is smaller than unity since a part of the dot wave functions lies outside the quantum well, when $\rho > R_0$, which reduces the splitting of the dot levels. The spin raising and lowering operators are defined as usual by $S^+_{\vec{R}} = S^x_{\vec{R}} + iS^y_{\vec{R}}$ and $S^-_{\vec{R}} = S^x_{\vec{R}} - iS^y_{\vec{R}}$, respectively.

The other important on-site interaction in QDs is the Coulomb repulsion between the charge carriers, which can be described by the following Hubbard Hamiltonian:[32,33]

$$\hat{H}_U = U\sum_{n,m,n',m',\sigma} \hat{n}_{nm\sigma}\hat{n}_{n'm'\bar{\sigma}}, \tag{12}$$

where U is the electron correlation parameter for the dot, $\hat{n}_{nm\sigma} = d^\dagger_{nm\sigma}d_{nm\sigma}$ is the occupation operator of the level $|nm\sigma\rangle$, and $\bar{\sigma}$ denotes the opposite spin direction to σ. By combining Eqs. (4), (7), and (12), we can write the final Hamiltonian for the isolated FSQD including the on-site exchange and Coulomb interactions,

$$\begin{aligned} \hat{H}_{\mathrm{FSQD}} &= \sum_{nm\sigma} E^{(1)}_{nm\sigma}d^\dagger_{nm\sigma}d_{nm\sigma} + \hat{V}_{sp\text{-}d} + \hat{H}_U \\ &= \hat{H}^{(1)}_{\mathrm{FSQD}} + \hat{V}_{sp\text{-}d} + \hat{H}_U, \end{aligned} \tag{13}$$

where

$$E^{(1)}_{nm\sigma} = E^0_{nm\sigma} - \frac{(\delta_{\sigma\uparrow} - \delta_{\sigma\downarrow})}{2}\Delta^{nm}_{sp\text{-}d} \tag{14}$$

is the energy of the spin-polarized dot level including the giant Zeeman splitting (10).

The FSQD is coupled to the nonmagnetic leads by tunneling processes, as shown in Fig. 1. The Hamiltonian for the charge carriers in the current leads is given by

$$\hat{H}_C = \sum_{\substack{\vec{k}\in L,R \\ \sigma}} \varepsilon_{\vec{k}\sigma}c^\dagger_{\vec{k}\sigma}c_{\vec{k}\sigma}, \tag{15}$$

where $c^\dagger_{\vec{k}\sigma}(c_{\vec{k}\sigma})$ creates (destroys) a spin-σ charge carrier with momentum $\vec{k}$ and energy $\varepsilon_{\vec{k}\sigma}$ in one of the leads on the right (R) or left (L). Finally, the tunneling of the charge carriers between the FSQD and the leads can be described by the following Hamiltonian:

$$\begin{aligned} \hat{H}_T = & \sum_{\substack{\vec{k}\in L \\ n,m,\sigma}} \langle\vec{k}\sigma|V_L(\vec{r})|nm\sigma\rangle c^\dagger_{\vec{k}\sigma}d_{nm\sigma} + \sum_{\substack{\vec{k}\in L \\ n,m,\sigma}} \langle nm\sigma|V_L(\vec{r}) \\ & \times|\vec{k}\sigma\rangle d^\dagger_{nm\sigma}c_{\vec{k}\sigma} + \sum_{\substack{\vec{k}\in R \\ n,m,\sigma}} \langle\vec{k}\sigma|V_R(\vec{r})|nm\sigma\rangle c^\dagger_{\vec{k}\sigma}d_{nm\sigma} \\ & + \sum_{\substack{\vec{k}\in R \\ n,m,\sigma}} \langle nm\sigma|V_R(\vec{r})|\vec{k}\sigma\rangle d^\dagger_{nm\sigma}c_{\vec{k}\sigma}, \end{aligned} \tag{16}$$

where $V_{L(R)}(\vec{r})$ is the potential barrier on the left (right) side of the FSQD.

To summarize, we can combine the Hamiltonians (1), (12), (13), (15), and (16) and write the final model Hamiltonian for the interacting FSQD as

$$\hat{H}_{\rm tot} = \hat{H}^{(1)}_{\rm FSQD} + \hat{H}_C + \hat{H}_U + \hat{V}_{sp\text{-}d} + \hat{H}_T + H_M. \tag{17}$$

This Hamiltonian is the simplest one that includes the coupling between the leads and the FSQD and allows us to consider the interplay between the on-site Coulomb and exchange interactions on the FSQD. $\hat{H}_{\rm tot}$ also includes the famous Anderson Hamiltonian $\hat{H}_A = \hat{H}^0_{\rm QD} + \hat{H}_C + \hat{H}_U + \hat{H}_T$ for nonmagnetic QDs.[31–33]

III. RETARDED GREEN'S FUNCTION FOR THE FSQD

The spectral densities, which are needed in the calculation of the conductance, level occupations and spin accumulation, are obtainable from the retarded Green function for the FSQD.[32] It can be calculated, e.g., by means of Zubarev's double-time-Green's-function technique[53] [also called an equation of motion (EOM) method[56]]. Let us apply this method to the dot level fermion operators $d_{nm\sigma}$ and $d^\dagger_{nm\sigma}$ in the case of the total Hamiltonian (17). By calculating the commutator $[d_{nm\sigma}, \hat{H}_{\rm tot}]$, we get the following EOM for the dot Green's function $G_{nm\sigma}(\omega) = \langle\langle d_{nm\sigma}; d^\dagger_{nm\sigma}\rangle\rangle$:

$$\begin{aligned}(\hbar\omega - E^{(1)}_{nm\sigma})\langle\langle d_{nm\sigma}; d^\dagger_{nm\sigma}\rangle\rangle &= 1 + \sum_{\vec{k}\in L}\langle nm\sigma|V_L(\vec{r})|\vec{k}\sigma\rangle\langle\langle c_{\vec{k}\sigma}; d^\dagger_{nm\sigma}\rangle\rangle + \sum_{\vec{k}\in R}\langle nm\sigma|V_R(\vec{r})|\vec{k}\sigma\rangle\langle\langle c_{\vec{k}\sigma}; d^\dagger_{nm\sigma}\rangle\rangle \\ &- \frac{J_{sp\text{-}d}\Omega}{2}\sum_{n',m',\sigma',\vec{R}}\psi^*_{nm}(\vec{R})\psi_{n'm'}(\vec{R})[\langle\langle(S^z_{\vec{R}} - \langle S^z_{\vec{R}}\rangle)d_{n'm'\sigma'}; d^\dagger_{nm\sigma}\rangle\rangle(\delta_{\sigma\uparrow} - \delta_{\sigma\downarrow}) + \langle\langle S^-_{\vec{R}} d_{n'm'\downarrow}; d^\dagger_{nm\sigma}\rangle\rangle\delta_{\sigma\uparrow} \\ &+ \langle\langle S^+_{\vec{R}} d_{n'm'\uparrow}; d^\dagger_{nm\sigma}\rangle\rangle\delta_{\sigma\downarrow}] + U\langle\langle d_{nm\sigma}\hat{n}_{nm\bar{\sigma}}; d^\dagger_{nm\sigma}\rangle\rangle\delta_{\sigma\uparrow} + U\langle\langle \hat{n}_{nm\bar{\sigma}} d_{nm\sigma}; d^\dagger_{nm\sigma}\rangle\rangle\delta_{\sigma\downarrow},\end{aligned} \tag{18}$$

New Green's functions such as $\langle\langle c_{\vec{k}\sigma}; d^\dagger_{nm\sigma}\rangle\rangle$, $\langle\langle S^\alpha_{\vec{R}} d_{n'm'\sigma'}; d^\dagger_{nm\sigma}\rangle\rangle$ ($\alpha = +, -, z$), and $\langle\langle d_{nm\sigma}\hat{n}_{nm\bar{\sigma}}; d^\dagger_{nm\sigma}\rangle\rangle$ are generated in Eq. (18), for which new EOMs can be derived. As an example, let us consider the Green's function $\langle\langle S^-_{\vec{R}} d_{n'm'\downarrow}; d^\dagger_{nm\sigma}\rangle\rangle$. Here we have used the Hartree–Fock (HF) approximation to the higher order Green's function $U\langle\langle S^-_{\vec{R}}\hat{n}_{nm\uparrow} d_{nm\downarrow}; d^\dagger_{nm\downarrow}\rangle\rangle \approx U\langle\hat{n}_{nm\uparrow}\rangle\langle\langle S^-_{\vec{R}} d_{nm\downarrow}; d^\dagger_{nm\downarrow}\rangle\rangle$ and also the decoupling $\langle\langle S^-_{\vec{R}} S^+_{\vec{R}'} d_{n'm'\uparrow}; d^\dagger_{nm\uparrow}\rangle\rangle \approx \langle S^-_{\vec{R}} S^+_{\vec{R}'}\rangle\langle\langle d_{n'm'\uparrow}; d^\dagger_{nm\uparrow}\rangle\rangle$, where $\langle S^-_{\vec{R}} S^+_{\vec{R}'}\rangle$ is the spin pair correlation function. Furthermore, following the steps we have applied in the case ferromagnetic quantum wells,[57] we get

$$\langle\langle S^-_{\vec{R}} d_{n'm'\downarrow}; d^\dagger_{nm\downarrow}\rangle\rangle = -\frac{J_{sp\text{-}d}\Omega}{2}\sum_{n',m',\vec{R}'}\frac{\psi^*_{nm}(\vec{R}')\psi_{n'm'}(\vec{R}')\langle S^-_{\vec{R}} S^+_{\vec{R}'}\rangle}{[\hbar\omega - E_{n'm'\downarrow} - U\langle\hat{n}_{n'm'\uparrow}\rangle - \Sigma^T_{n'm'\downarrow}(\hbar\omega)]}\langle\langle d_{n'm'\uparrow}; d^\dagger_{nm\uparrow}\rangle\rangle, \tag{19}$$

where the self-energy for the tunneling processes is given by

$$\begin{aligned}\Sigma^T_{nm\sigma}(\hbar\omega) &= \sum_{\vec{k}\in L(R)}\frac{|\langle\vec{k}\sigma|V_{L(R)}(\vec{r})|nm\sigma\rangle|^2}{(\hbar\omega - \varepsilon_{\vec{k}\sigma})} \\ &= {\rm Re}\{\Sigma^T_{nm\sigma}(\hbar\omega)\} - i\frac{\Gamma(nm\sigma)}{2},\end{aligned} \tag{20}$$

with

$$\begin{aligned}\Gamma_{nm\sigma}(\hbar\omega) &= 2\pi\sum_{\vec{k}\in L}|\langle\vec{k}\sigma|V_L(\vec{r})|nm\sigma\rangle|^2\delta(\hbar\omega - \varepsilon_{\vec{k}\sigma}) \\ &+ 2\pi\sum_{\vec{k}\in R}|\langle\vec{k}\sigma|V_R(\vec{r})|nm\sigma\rangle|^2\delta(\hbar\omega - \varepsilon_{\vec{k}\sigma}) \\ &= \Gamma^L_{nm\sigma}(\hbar\omega) + \Gamma^R_{nm\sigma}(\hbar\omega).\end{aligned} \tag{21}$$

In the same way, the EOMs for the other higher order Green's functions $\langle\langle S^\alpha_{\vec{R}} d_{nm\sigma}; d^\dagger_{nm\sigma}\rangle\rangle$ with $\alpha = +$ or z can be derived. The solutions are similar to Eq. (19) when the spin-correlation function $\langle S^-_{\vec{R}} S^+_{\vec{R}}\rangle$ is replaced by the functions $\langle S^+_{\vec{R}} S^-_{\vec{R}'}\rangle$ and $\langle(S^z_{\vec{R}} - \langle S^z_{\vec{R}}\rangle)(S^z_{\vec{R}'} - \langle S^z_{\vec{R}'}\rangle)\rangle$ for $\alpha = +$ and z, respectively.

The spin operator dependent higher order Green's functions (19) appear also in the EOMs for the Green's functions $\langle\langle d_{nm\downarrow}\hat{n}_{nm\downarrow}; d^\dagger_{nm\downarrow}\rangle\rangle$ and $\langle\langle\hat{n}_{nm\uparrow} d_{nm\downarrow}; d^\dagger_{nm\downarrow}\rangle\rangle$ generated in Eq. (18), for which we find

$$\begin{aligned}&[\hbar\omega - E^{(1)}_{nm\uparrow} - U]\langle\langle d_{nm\uparrow}\hat{n}_{nm\downarrow}; d^\dagger_{nm\uparrow}\rangle\rangle \\ &= \langle\hat{n}_{nm\downarrow}\rangle + \sum_{\vec{k}\in L(R)}\langle nm\uparrow|V_{L(R)}(\vec{r})|\vec{k}\uparrow\rangle\langle\hat{n}_{nm\downarrow}\rangle\langle\langle c_{\vec{k}\uparrow}; d^\dagger_{nm\uparrow}\rangle\rangle \\ &- \left(\frac{J_{sp\text{-}d}\Omega\langle\hat{n}_{nm\downarrow}\rangle}{2}\right)\sum_{n'm'\vec{R}}\psi^*_{nm}(\vec{R})\psi_{n'm'}(\vec{R}) \\ &\times[\langle\langle S^-_{\vec{R}} d_{n'm'\downarrow}; d^\dagger_{nm\downarrow}\rangle\rangle + \langle\langle(S^z_{\vec{R}} - \langle S^z_{\vec{R}}\rangle)' d_{n'm'\uparrow}; d^\dagger_{nm\uparrow}\rangle\rangle].\end{aligned} \tag{22}$$

Inserting Eq. (19) into Eq. (22) we can solve Eq. (22) and a similar EOM for the Green's function $\langle\langle \hat{n}_{nm\uparrow} d_{nm\downarrow}; d^{\dagger}_{nm\sigma}\rangle\rangle$ and obtain

$$\langle\langle d_{nm\uparrow}\hat{n}_{nm\downarrow}; d^{\dagger}_{nm\uparrow}\rangle\rangle = \frac{\langle \hat{n}_{nm\downarrow}\rangle[1+\Sigma^{(2)}_{\mathrm{tot}}(\hbar\omega, nm\uparrow)\langle\langle d_{nm\uparrow}; d^{\dagger}_{nm\uparrow}\rangle\rangle]}{[\hbar\omega - E^{(1)}_{nm\uparrow} - U]}, \tag{23}$$

and

$$\langle\langle \hat{n}_{nm\uparrow} d_{nm\downarrow}; d^{\dagger}_{nm\downarrow}\rangle\rangle = \frac{\langle \hat{n}_{nm\uparrow}\rangle[1+\Sigma^{(2)}_{\mathrm{tot}}(\hbar\omega, nm\downarrow)\langle\langle d_{nm\downarrow}; d^{\dagger}_{nm\downarrow}\rangle\rangle]}{[\hbar\omega - E^{(1)}_{nm\downarrow} - U]}, \tag{24}$$

where $\Sigma^{(2)}_{\mathrm{tot}}(\hbar\omega, nm\sigma) = \Sigma^{T}_{nm\sigma}(\hbar\omega) + \Sigma^{(2)}_{sp\text{-}d}(\hbar\omega, nm\sigma)$ is the total self-energy including the tunneling processes and the *sp-d* exchange interaction. Here $\Sigma^{(2)}_{sp\text{-}d}(\hbar\omega, nm\sigma)$ is the second order self-energy related to $\hat{V}_{sp\text{-}d}$, which is given by

$$\Sigma^{(2)}_{sp\text{-}d}(\hbar\omega, nm\sigma) = \left(\frac{J_{sp\text{-}d}\Omega}{2}\right)^2 \sum_{n'm'\vec{R},\vec{R}'} \psi^{*}_{nm}(\vec{R})\psi_{n'm'}(\vec{R})\psi^{*}_{n'm'}(\vec{R}')\psi_{nm}(\vec{R}') \cdot \left\{ \frac{\langle S^{+}_{\vec{R}} S^{-}_{\vec{R}'}\rangle \delta_{\sigma\downarrow}}{\hbar\omega - E^{(1)}_{n'm'\uparrow} - U\langle \hat{n}_{n'm'\downarrow}\rangle - \Sigma^{T}_{nm\downarrow}} + \frac{\langle S^{-}_{\vec{R}} S^{+}_{\vec{R}'}\rangle \delta_{\sigma\uparrow}}{\hbar\omega - E^{(1)}_{n'm'\downarrow} - U\langle \hat{n}_{n'm'\uparrow}\rangle - \Sigma^{T}_{nm\uparrow}} + \frac{\langle (S^{z}_{\vec{R}} - \langle S^{z}_{\vec{R}}\rangle)(S^{z}_{\vec{R}'} - \langle S^{z}_{\vec{R}'}\rangle)\rangle}{\hbar\omega - E^{(1)}_{n'm'\sigma} - \Sigma^{T}_{nm\sigma}} \right\}. \tag{25}$$

Now we can solve our original EOM (18) by inserting Eqs. (19), (23), and (24) into Eq. (18), and finally, we obtain the retarded Green's function for the FSQD,

$$G^{(2)}_{nm\sigma}(\hbar\omega) = \langle\langle d_{nm\sigma}; d^{\dagger}_{nm\sigma}\rangle\rangle = \frac{\hbar\omega - E^{(1)}_{nm\sigma} - U(1-\langle \hat{n}_{nm\bar{\sigma}}\rangle)}{(\hbar\omega - E^{(1)}_{nm\sigma})(\hbar\omega - E^{(1)}_{nm\sigma} - U) - \Sigma^{(2)}_{\mathrm{tot}}(\hbar\omega, nm\sigma)[\hbar\omega - E^{(1)}_{nm\sigma} - U(1-\langle \hat{n}_{nm\bar{\sigma}}\rangle)]}, \tag{26}$$

This result is similar to the one obtained for the nonmagnetic QDs,[56,58] excluding correction (25) related to the *sp-d* interaction.

In the diluted magnetic semiconductors, the *sp-d* exchange interaction is very large[2,20] causing strong spin-disorder scattering at temperatures close to T_C. Also the spin-correlation functions $\langle S^{\alpha}_{\vec{R}} S^{\alpha'}_{\vec{R}'}\rangle$ appearing in the self-energy (25) are divergent in the long-wavelength limit at T_C (see Sec. IV B). Therefore, as shown by Sinkkonen,[59] the weak-coupling theory is not valid anymore, and the self-energy related to the *sp-d* interaction must be calculated in a self-consistent manner using an infinite order perturbation theory. In the calculation of the self-energy $\Sigma_{sp\text{-}d}$, we can apply Sinkkonen's method,[59] which is equivalent to the well-known self-consistent Born approximation (SCBA).[58] In our case it means that we continue the chain of EOMs for the higher order Green's functions such as Eq. (19) to infinite order. Taking into account only the two-spin-correlation functions, the summation of the perturbation expansion can be performed, and we get an expression for the self-energy similar to Eq. (25). However, now the self-energy appears also in the denominator, and we obtain the following self-consistent equation:

$$\Sigma^{\mathrm{SCBA}}_{sp\text{-}d}(\hbar\omega, nm\sigma) = \left(\frac{J_{sp\text{-}d}\Omega}{2}\right)^2 \sum_{n'm'\vec{R},\vec{R}'} \psi^{*}_{nm}(\vec{R})\psi_{n'm'}(\vec{R})\psi^{*}_{n'm'}(\vec{R}')\psi_{nm}(\vec{R}') \cdot \left\{ \frac{\langle S^{+}_{\vec{R}} S^{-}_{\vec{R}'}\rangle \delta_{\sigma\downarrow}}{\hbar\omega - E^{(1)}_{n'm'\uparrow} - U\langle \hat{n}_{n'm'\downarrow}\rangle - \Sigma^{T}_{nm\downarrow} - \Sigma^{\mathrm{SCBA}}_{sp\text{-}d}(\hbar\omega, nm\sigma)} + \frac{\langle S^{-}_{\vec{R}} S^{+}_{\vec{R}'}\rangle \delta_{\sigma\uparrow}}{\hbar\omega - E^{(1)}_{n'm'\downarrow} - U\langle \hat{n}_{n'm'\uparrow}\rangle - \Sigma^{T}_{nm\uparrow} - \Sigma^{\mathrm{SCBA}}_{sp\text{-}d}(\hbar\omega, nm\sigma)} + \frac{\langle (S^{z}_{\vec{R}} - \langle S^{z}_{\vec{R}}\rangle)(S^{z}_{\vec{R}'} - \langle S^{z}_{\vec{R}'}\rangle)\rangle}{\hbar\omega - E^{(1)}_{n'm'\sigma} - \Sigma^{T}_{nm\sigma} - \Sigma^{\mathrm{SCBA}}_{sp\text{-}d}} \right\}, \tag{27}$$

Furthermore, in SCBA the retarded Green's function (26) can be expressed in a compact form as

$$G^{\mathrm{SCBA}}_{nm\sigma}(\hbar\omega) = \frac{1-\langle \hat{n}_{nm\sigma}\rangle}{\hbar\omega - E^{(1)}_{nm\sigma} - \Sigma^{\mathrm{SCBA}}_{\mathrm{tot}}(\hbar\omega, nm\sigma)} + \frac{\langle \hat{n}_{nm\sigma}\rangle}{\hbar\omega - E^{(1)}_{nm\sigma} - \Sigma^{\mathrm{SCBA}}_{\mathrm{tot}}(\hbar\omega, nm\sigma) - U}, \tag{28}$$

where

$$\Sigma^{\mathrm{SCBA}}_{\mathrm{tot}}(\hbar\omega, nm\sigma) = \Sigma^{T}_{nm\sigma}(\hbar\omega) + \Sigma^{\mathrm{SCBA}}_{sp\text{-}d}(\hbar\omega, nm\sigma). \tag{29}$$

We find, as in the case of nonmagnetic QDs,[32] that $G^{\mathrm{SCBA}}_{nm\sigma}(\hbar\omega)$ has two resonances, one at $\hbar\omega = E^{(1)}_{nm\sigma} + \Sigma^{\mathrm{SCBA}}_{\mathrm{tot}}(\hbar\omega, nm\sigma)$ weighted by the probability $1-\langle \hat{n}_{nm\sigma}\rangle$ that the other level is vacant and the other one at $\hbar\omega = E^{(1)}_{nm\sigma} + \Sigma^{\mathrm{SCBA}}_{\mathrm{tot}}(\hbar\omega, nm\sigma) + U$ weighted by the probability $\langle \hat{n}_{nm\sigma}\rangle$ that the other level is occupied. However, in the case of the FSQD, there is an additional renormalization of the dot levels by $\mathrm{Re}\{\Sigma^{\mathrm{SCBA}}_{nm\sigma}\}$ as well as a level broadening

$\mathrm{Im}\{\Sigma^{\mathrm{SCBA}}_{nm\sigma}\}$ due to the *sp-d* exchange interaction. The quantity $\mathrm{Im}\{\Sigma^{\mathrm{SCBA}}_{sp\text{-}d}\}/\hbar$ can be interpreted as a scattering rate for the spin-disorder scattering,[55] where the first two terms in Eq. (27) describe the spin-flip processes $\bar{\sigma}=\downarrow \rightarrow \sigma=\uparrow$ and $\sigma=\uparrow \rightarrow \bar{\sigma}=\downarrow$, respectively, and the last term is related to the transitions without any spin flip. An interesting fact is the appearance of the terms $U\langle \hat{n}_{nm\sigma}\rangle$ in the denominator of Eq. (27) as a consequence of the HF approximation in the derivation of the higher order Green's functions. Therefore, the self-energy and the occupation probabilities must be calculated in a self-consistent manner. We have used the HF approximation only for the spin-flip terms in the derivation of Eq. (27), since in the case of the transitions without spin-flips we will consider only the transitions within the broadened dot level (see Sec. IV). The self-energy (27) and the Green's function (28) are the main results of the present work, which allow us to estimate the spectral densities and the conductance in a FSQD as a function of temperature and external magnetic field.

IV. NUMERICAL RESULTS AND DISCUSSION

A. Parameters

In order to simplify the calculations and to see clearly the effect of the *sp-d* exchange interaction on the properties of the FSQD, we assume that the dot consists only of a single spin-degenerate energy level $\varepsilon_{d\sigma} \equiv E^{(1)}_{nm\sigma}$, given by Eq. (14), on which there is the Coulomb interaction U, as shown in Fig. 1. Here $\varepsilon_{d\sigma}$ denotes the topmost occupied level of the dot, which we consider responsible for transport. All other energy levels $E^{(1)}_{n'm'\sigma}$ of the dot are neglected since we assumed that they do not take part in transport. Therefore, in our model FSQD we have only four different energy levels denoted by $\varepsilon_1(\uparrow)=\varepsilon_{d\uparrow}=E^0_{nm}-\Delta^d_{sp\text{-}d}/2$, $\varepsilon_2(\downarrow)=\varepsilon_{d\downarrow}=E^0_{nm}+\Delta^d_{sp\text{-}d}/2$, $\varepsilon_3(\uparrow)=\varepsilon_{d\uparrow}+U=E^0_{nm}-\Delta^d_{sp\text{-}d}/2+U$, and $\varepsilon_4(\downarrow)=\varepsilon_{d\downarrow}+U=E^0_{nm}+\Delta^d_{sp\text{-}d}/2+U$ (see Fig. 1), when the spin degeneracy is removed due to the giant Zeeman splitting $\Delta_{sp\text{-}d}=xJ^{sp\text{-}d}_{\mathrm{exch}}\langle S^z\rangle F_{00}=\varepsilon_2(\downarrow)-\varepsilon_1(\uparrow)=\varepsilon_4(\downarrow)-\varepsilon_3(\uparrow)$ in the case of a nonvanishing spin polarization $\langle S^z\rangle$ of the magnetic ions. Here we have neglected the ordinary Zeeman splitting since at the magnetic fields studied in the present paper it is orders of magnitude smaller than $\Delta^d_{sp\text{-}d}$. Furthermore, we assume that F_{00} can be calculated from Eq. (11) for the ground state wave function[54] ψ_{00} given by

$$\psi_{00}(\rho,z)=\left(\frac{\sqrt{2}}{l_\omega\sqrt{\pi z_0}}\right)\sin\left[\frac{\pi}{z_0}\left(z+\frac{z_0}{2}\right)\right]e^{-\rho/2l_\omega}, \qquad (30)$$

where l_w describes the decay of the wave function. We consider a rather small dot with dimensions $R_0=z_0=10$ nm, for which the charging energy U can be estimated using the first order perturbation theory for the Coulomb interaction $W_{ee}=e^2/4\pi\varepsilon r$ between the two electron on the dot, $U=\langle 00|W_{ee}|00\rangle \approx 30$ meV.[54] However, in the calculations below, we vary the value of U between 5 and 50 meV since the size of the QDs can be varied in the fabricated dots. The other material parameters were those of diluted III-V magnetic semiconductors, such as Mn-doped GaAs: $a_0=5.65$ Å, $x=0.04$, $T_C=30-50$ K, $m^*=0.5m_0$, and $S=5/2$. One of the most interesting parameters for FSQDs is the *sp-d* exchange interaction parameter $J_{sp\text{-}d}$, for which the experimental values vary a lot. In the case of the electrons the estimates range from 0.023 (Ref. 60) to 0.18–0.26 eV,[61] and in the case of holes from 0.6 (Ref. 62) to 2.5 ± 0.8 eV.[63] In the present work, we have chosen mainly the lower values, i.e, $J_{s\text{-}d}=0.1$ eV for electrons and $J_{p\text{-}d}=0.8$ eV for holes, in order to compensate partly for the too large values of the spin-correlation functions for FSQDs, when they are estimated from the results derived for bulk ferromagnets in the long-wavelength limit (see Sec. IV B). For the coupling parameter Γ, we use the constant value of 0.5 meV for all the dot levels (a wide-band limit) symmetrically on both sides of the FSQD.

B. Spin correlation functions

The experimental results[29] for magnetization vs temperature show that the FSQDs behave qualitatively according to the predictions of the mean-field theory. Therefore, we have estimated the average spin polarization of the magnetic atoms inside a FSQD from Hamiltonian (1) within the molecular field approximation (MFA),[59,63,64] which yields

$$x\langle S^z\rangle = N^{-1}\sum_{\vec{R}}\langle S^z_{\vec{R}}\rangle = xSB_S(\eta). \qquad (31)$$

Here $B_S(\eta)$ is the Brillouin function for the spin quantum number S of the magnetic atoms and

$$\eta=\frac{g_L\mu_B S}{k_BT}B_{\mathrm{eff}}=\frac{g_L\mu_B S}{k_BT}\left[B+\frac{3k_BT_C}{S(S+1)g_L\mu_B}\langle S^z\rangle\right], \qquad (32)$$

where B_{eff} is the effective molecular field acting on the spin $\vec{S}_{\vec{R}}$. There is no theory of spin fluctuations in small magnetic quantum dots having a limited number of magnetic ions. Although the measured average magnetization[29] in small FSQDs behaves according to the mean-field theory, we have no guarantee that the spin pair correlations act as those in the bulk ferromagnets. Especially, we may expect that in the case of the FSQDs made of the diluted magnetic semiconductors, the ferromagnetism is more complex than in bulk due to, e.g., the epitaxial strain, substitutional disorder, quantum confinement, clustering of the magnetic atoms, carrier induced ferromagnetic coupling, and bound magnetic polarons. All these effects may suppress the spin fluctuations in QDs compared to those in bulk. However, in spite of all these effects, we believe that at least a qualitatively correct behavior (i.e., a peak at T_C and a suppression of fluctuations with external magnetic field) can be found using MFA in the derivation of the spin pair correlation functions if we take into account the substitutional disorder, i.e, the fact that a magnetic atom is found at a lattice site $\vec{R}$ with probability x. Then we can apply the method developed by Sinkkonen[59,63] and later refined by Takahashi *et al.*[65] for the calculation of the temperature and magnetic field dependence of the spin-correlation functions $\langle S^\alpha_{\vec{R}} S^{\alpha'}_{\vec{R}'}\rangle$ needed in the self-energy (27). The expressions in the long-wavelength limit are given by

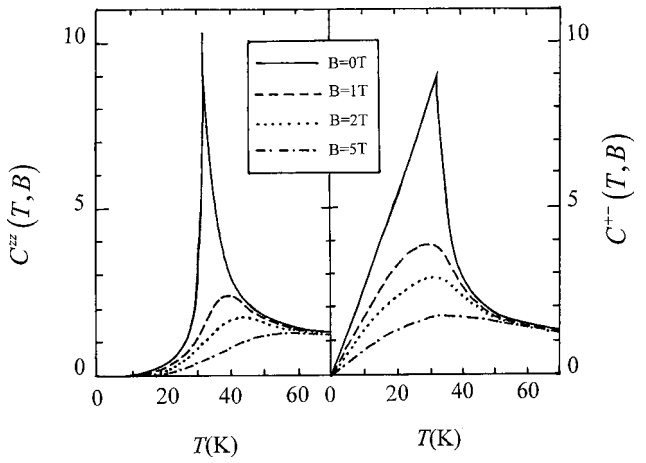

FIG. 2. Transverse and longitudinal spin-correlation function $C^{+-}=C^{-+}$ and C^{zz}, respectively, vs temperature at various external magnetic fields in a FSQD with $T_C=30$ K.

$$C^{-+}(T,B)=C^{+-}(T,B)=\frac{\kappa(T)xTS^2B_S(\eta)/\eta}{T-\frac{3ST_CB_S(\eta)}{\eta(S+1)}}, \tag{33}$$

$$C^{zz}(T,B)=\frac{\kappa(T)xTS^2\,\partial B_S(\eta)/\partial\eta}{T-\frac{3ST_C\,\partial B_S(\eta)/\partial\eta}{(S+1)}}, \tag{34}$$

where $C^{\alpha\alpha'}(T,B)=\lim_{q\to 0}\langle S^{\alpha}_{\vec{R}}S^{\alpha'}_{\vec{R}'}\rangle_q$ and $\langle S^{\alpha}_{\vec{R}}S^{\alpha'}_{\vec{R}'}\rangle_q$ is the Fourier transform of the spin-correlation function with $\alpha,\alpha'=+,-,z$. $\kappa(T)$ is a weakly temperature dependent factor which has the value of 0.5 at temperatures close to T_C and then increases slightly at higher temperatures.[65] We have used the constant value of 0.5 in all our numerical calculations since we are mainly interested in the behavior of the FSQDs in the temperature region where the spin fluctuations are largest, i.e., when $T\approx T_C$. Using a Taylor expansion for the Brillouin function $B_S(\eta)\approx(S+1)\eta/3S$, when $\eta\ll 1$, we find that the spin-correlation functions (33) and (34) diverge at $T=T_C$, $C^{\alpha\alpha'}(T)\sim 1/|T-T_C|$, which was the motivation for the use of the infinite order perturbation theory[59] in the derivation of the expression for the self-energy (27).

Figure 2 shows the transverse and longitudinal spin pair correlation functions (33) and (34), respectively, vs temperature at various magnetic fields in a FSQD, when the Curie temperature is 30 K. The main difference between the two functions is found at low temperatures $T<T_C$, where the transverse correlation function $C^{+-}(T,B)$ [and $C^{-+}(T,B)$] is much larger than the longitudinal function $C^{zz}(T,B)$. An important feature is the large magnetic field dependence of the correlation functions at temperatures close to T_C, i.e., the spin fluctuations are suppressed strongly by an increasing magnetic field. Although expressions (33) and (34) may overestimate the magnitude of the spin fluctuations, we believe that a detailed theory for the spin correlations in a small FSQD would preserve the main features of $C^{\alpha\alpha'}(T,B)$, i.e., the strong peak at $T=T_C$ and the decrease of the spin fluctuations with increasing magnetic ordering.

C. Spectral densities and level broadening

The spectral densities for a FSQD can be expressed in terms of the dot Green's function (28), and they are given by

$$A_{d\sigma}(\omega)=-\frac{1}{\pi}\mathrm{Im}\{G^{\mathrm{SCBA}}_{d\sigma}(\hbar\omega+i\varepsilon)\}. \tag{35}$$

On the other hand, the Green's function $G^{\mathrm{SCBA}}_{d\sigma}$ depends on the occupation probabilities $\langle\hat{n}_\sigma\rangle$, which are given by an integral of the spectral density weighted by the Fermi factor $n_F(\omega)$,

$$\langle\hat{n}_{d\sigma}\rangle=\int d\omega n_F(\omega)A_{d\sigma}(\omega). \tag{36}$$

Furthermore, using the correlation functions (33) and (34), we can estimate the level broadening γ_i^{SCBA} for the level $\varepsilon_i(\sigma)$ from the imaginary part of the self-energy (27), and it is given by

$$\begin{aligned}\gamma_i^{\mathrm{SCBA}}[\varepsilon_i(\sigma)]&=\mathrm{Im}\{\Sigma^{\mathrm{SCBA}}_{sp\text{-}d}[\varepsilon_i(\sigma)]\}\\&=\left(\frac{J_{sp\text{-}d}\Omega F_{00}}{2}\right)^2\\&\times\left\{\frac{C^{+-}(T,B)\gamma^{\mathrm{tot}}_{i\sigma}\delta_{\sigma\downarrow}}{[\varepsilon_i(\downarrow)-\tilde{\varepsilon}_{d\uparrow}-U\langle\hat{n}_{d\uparrow}\rangle]^2+(\gamma^{\mathrm{tot}}_{i\sigma})^2}\right.\\&+\frac{C^{-+}(T,B)\gamma^{\mathrm{tot}}_{i\sigma}\delta_{\sigma\uparrow}}{[\varepsilon_i(\uparrow)-\tilde{\varepsilon}_{d\downarrow}-U\langle\hat{n}_{d\downarrow}\rangle]^2+(\gamma^{\mathrm{tot}}_{i\sigma})^2}\\&\left.+\frac{C^{zz}(T,B)\gamma^{\mathrm{tot}}_{i\sigma}}{[\varepsilon_i(\sigma)-\tilde{\varepsilon}_{d\sigma}]^2+(\gamma^{\mathrm{tot}}_{i\sigma})^2}\right\},\end{aligned} \tag{37}$$

where $\gamma^{\mathrm{tot}}_{i\sigma}=\gamma_i^{\mathrm{SCBA}}[\varepsilon_i(\sigma)]+\Gamma/2$ is the total level broadening including both spin-disorder scattering and tunneling, and

$$\begin{aligned}\tilde{\varepsilon}_{d\sigma}&=E^0_{nm\sigma}+\mathrm{Re}\{\Sigma^{\mathrm{SCBA}}_{sp\text{-}d}\}+\mathrm{Re}\{\Sigma_T\}-\frac{\Delta^d_{sp\text{-}d}}{2}(\delta_{\sigma\uparrow}-\delta_{\sigma\downarrow})\\&\equiv\tilde{\varepsilon}_d-\frac{\Delta^d_{sp\text{-}d}}{2}(\delta_{\sigma\uparrow}-\delta_{\sigma\downarrow}).\end{aligned} \tag{38}$$

We have solved Eqs. (35)–(38) self-consistently by iterations. For the spin-flip processes in Eq. (37), we have considered transitions between the dot levels having opposite spins, such as the transition from $\varepsilon_1(\uparrow)$ to $\varepsilon_2(\downarrow)$, but for the transitions without spin-flips only those which occur within the broadened level. This is possible, when the level broadening is calculated self-consistently from Eq. (37). Figure 3 summarizes the behavior of the spectral density $A_{d\uparrow}(\omega)$ for spin-up electrons in a FSQSD with the parameters $T_C=30$ K, $x=0.04$, $U=40$ meV, $J^{s\text{-}d}_{\mathrm{exch}}=0.1$ eV, and $l_w=0.7$ nm. The results for the spin-down electrons are mirror images of those in Fig. 3 with respect to the energy $\hbar\omega=\tilde{\varepsilon}_d+U/2$ (particle-hole symmetry[33]). At low temperatures $T<T_C$, where the spin fluctuations are small, there are two resonances at $\hbar\omega\approx\tilde{\varepsilon}_d$ and $\hbar\omega\approx\tilde{\varepsilon}_d+U$. At $T\approx T_C$ the large

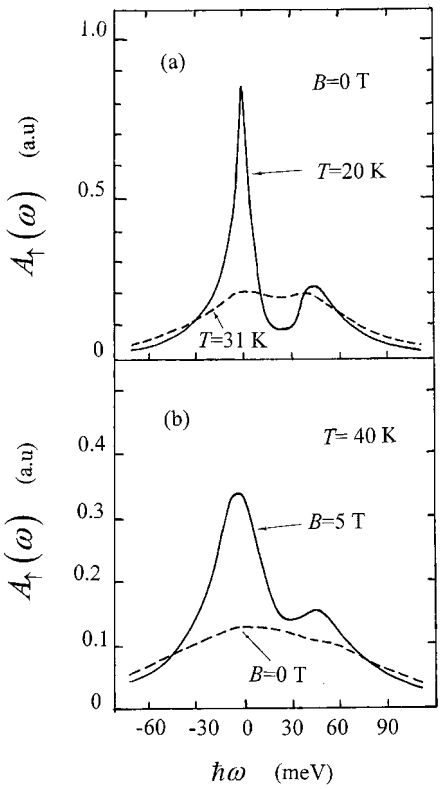

FIG. 3. Spectral density $A_{d\uparrow}(\omega)$ vs $\hbar\omega$ in a FSQD with T_C =30 K, x=0.04, U=40 meV, and $J^{s\text{-}d}_{\text{exch}}$=0.1 eV (a) at two temperatures (B=0 T) and (b) at two magnetic fields (T=40 K).

spin fluctuations, and consequently, the large level broadenings (see below) decrease and broaden the resonance peaks. On the other hand, even at $T>T_C$ a magnetic field restores the resonance peaks due to decreasing level broadening with increasing magnetic field.

Figure 4 shows the calculated level broadenings γ_1 =Im$\{\Sigma^{\text{SCBA}}_{\text{exch}}[\varepsilon_1(\uparrow)]\}$ and γ_2=Im$\{\Sigma^{\text{SCBA}}_{\text{exch}}[\varepsilon_2(\downarrow)]\}$ as a function of temperature at various magnetic fields. The results for

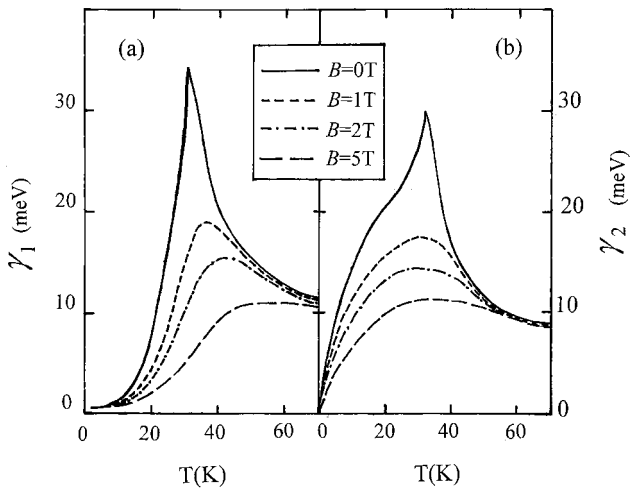

FIG. 4. The level broadenings γ_1=Im$\{\Sigma^{\text{SCBA}}_{\text{exch}}[\varepsilon_1(\uparrow)]\}$ and γ_2 =Im$\{\Sigma^{\text{SCBA}}_{\text{exch}}[\varepsilon_2(\downarrow)]\}$ vs temperature at various magnetic fields in a FSQD. The results for $\gamma_3(\gamma_4)$ were similar to those of x $\gamma_3(\gamma_4)$. The parameters are the same as in Fig. 3.

$\gamma_3(\gamma_4)$ are similar to those of $\gamma_2(\gamma_1)$. The level broadening is very large as compared to the coupling constant Γ, even with a rather small value for the exchange interaction parameter $J_{sp\text{-}d}$=0.1 eV. The large values for γ_i are related to an overestimation of the spin-correlation functions (33) and (34), when they are calculated in the long-wavelength limit. However, this overestimation is not a problem in our case since for the conclusions from the conductance results below, the most important factor is the ratio $J_{sp\text{-}d}/U$, which can be adjusted in FSQDs quite freely by changing the size of the dot and thereby changing the Coulomb repulsion U.

The strong temperature and magnetic field dependences of the level broadenings in Fig. 4 are due to the T and B dependences of the spin-correlation functions $C^{\alpha\alpha'}(T,B)$ (see Fig. 2). At temperatures close to T_C, the level broadenings are on the same order of magnitude as the charging energy U. At low temperatures $T<T_C$, γ_2 is larger than γ_1 since in this temperature range the spin-flip processes between the broadened dot levels dominate in γ_2, where as in γ_1 the transitions within the broadened levels without spin-flip are more important. More precisely, in the case of the spin-flip processes for γ_1 and γ_2, we get $|\hbar\omega-\tilde{\varepsilon}_d-U\langle\hat{n}_{d\downarrow}\rangle|$ $=|\Delta^d_{sp\text{-}d}+U\langle\hat{n}_{d\downarrow}\rangle|$ with $\hbar\omega=\varepsilon_1(\uparrow)=\tilde{\varepsilon}_d-\Delta^d_{sp\text{-}d}/2$ and $|\hbar\omega-\tilde{\varepsilon}_d-U\langle\hat{n}_{d\uparrow}\rangle|=|\Delta^d_{sp\text{-}d}-U\langle\hat{n}_{d\uparrow}\rangle|$ with $\hbar\omega$ $=\varepsilon_2(\downarrow)=\tilde{\varepsilon}_d+\Delta^d_{sp\text{-}d}/2$, respectively, in the denominators of Eq. (37). Therefore, with the increasing Zeeman splitting $\Delta^d_{sp\text{-}d}$ at $T<T_C$, $\gamma_1\sim(\Delta^d_{sp\text{-}d}+U\langle\hat{n}_{d\downarrow}\rangle)^{-2}$ decreases, whereas γ_2 $\sim(\Delta^d_{sp\text{-}d}-U\langle\hat{n}_{d\uparrow}\rangle)^{-2}$ increases, especially if $\Delta^d_{sp\text{-}d}\approx U\langle\hat{n}_{d\uparrow}\rangle$. This condition can also be interpreted as a spin-flip resonance between the levels $\varepsilon_2(\downarrow)$ and $\varepsilon_3(\uparrow)$. The spin-flip processes are improbable during the double occupancy of the dot since, e.g., the transition from $\varepsilon_1(\uparrow)$ to $\varepsilon_2(\downarrow)$ is forbidden if $\langle\hat{n}_{d\uparrow}\rangle=\langle\hat{n}_{d\downarrow}\rangle=1$. However, in the case where the Fermi energy lies between $\tilde{\varepsilon}_d$ and $\tilde{\varepsilon}_d+U$ and where also the large conductance resonance is seen, we find that on the average the dot is singly occupied with $\langle\hat{n}_{d\uparrow}\rangle\approx\langle\hat{n}_{d\downarrow}\rangle\approx0.5$ (see Sec. IV E). This is a finding previously reported in the case of the Kondo resonance.[31] The intradot spin-flip scattering in nonmagnetic QDs due to spin-orbit coupling has been discussed by several groups[48–51] using phenomenological models. In our model (27) both the spin-flip and nonflipping processes are treated using a microscopic theory.

D. Conductance

The linear magnetoconductance $g=\lim_{V\to0}\partial I/\partial V$ through a QD can be calculated using a Landauer-type formula[32,33] generalized to interacting systems in the wide-band limit,

$$g(T,B)=\frac{e^2}{\hbar^2}\frac{\Gamma_L\Gamma_R}{\Gamma_L+\Gamma_R}\sum_\sigma\int_{-\infty}^{\infty}d\varepsilon A_{d\sigma}(\varepsilon,T,B)\left(-\frac{\partial n_F(\varepsilon)}{\partial\varepsilon}\right), \tag{39}$$

Figure 5 shows the conductance vs Fermi energy (or gate voltage eV_g) at 4 K$\ll T_C$ and at B=0 T for various values of the Coulomb repulsion U. The other parameters are the same as in Fig. 3. When U=5 meV or less, there is only a single peak and no CB effect. This is due to the fact even at 4 K the level broadening γ_2 (and γ_3), shown in Fig. 4, is on the same

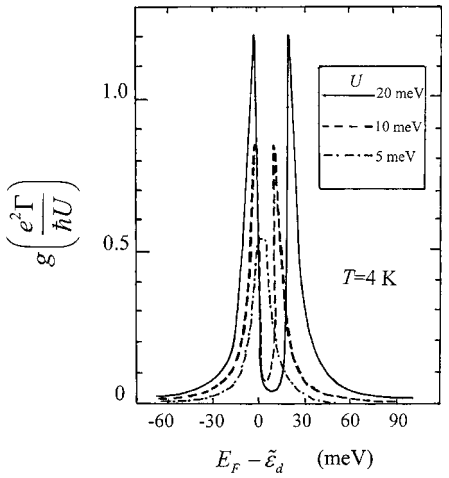

FIG. 5. Conductance, in units of $(\Gamma/U)(e^2/\hbar)$, vs energy difference between the Fermi level E_F and the dot level $\tilde{\varepsilon}_d$ (or vs gate voltage) at $T=4$ K with various values for U when $B=0$ T. The other parameters are the same as in Fig. 3.

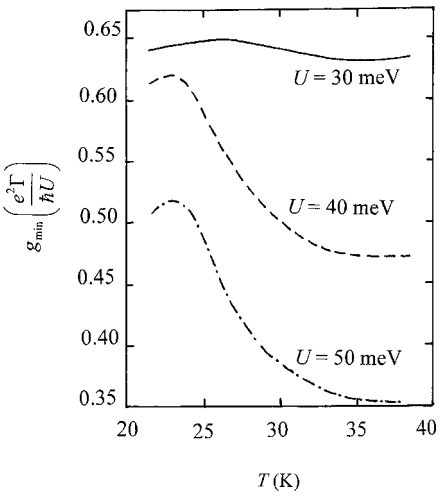

FIG. 7. Temperature dependence of the conductance minimum, in units of $(\Gamma/U)(e^2/\hbar)$, at $E_F-\tilde{\varepsilon}_d=20$ meV between the two conductance peaks for various values of U. The parameters are the same as in Fig. 3.

order of magnitude as U, which washes out the sharp resonances. For larger values of U, the ordinary CB effect can be seen, and the separation of the two conductance peaks depends on the value of U. Although the bare level spacing is $\Delta^d_{sp\text{-}d}$ so that even if there in principle are four energy levels in the FSQD at $T<T_C$, as shown in Fig. 1, only two peaks appear in the conductance, split by $U+\Delta^d_{sp\text{-}d}$. This suppression of peaks follows from the dependence of the spectral density of each level on the occupancy of the other level, as reported previously by Meir *et al.*[32]

The CB effect, which is shown clearly at low temperatures $T<T_C=30$ K, almost vanishes, when T approaches T_C [Figs. 6(a) and 6(b)]. This is due to the large increase in the level broadenings γ_i at temperatures close to T_C, as shown in Fig. 2, which causes an increasing overlap between the spectral densities of the bare dot levels. At $T>T_C$ the CB effect becomes more clear again due to the decreasing level broadenings shown in Fig. 2, which makes the conductance peaks sharper. However, at $T\geq 150$ K$\gg T_C$ the thermal effects wash out the CB effect, as shown in Fig. 6(b).

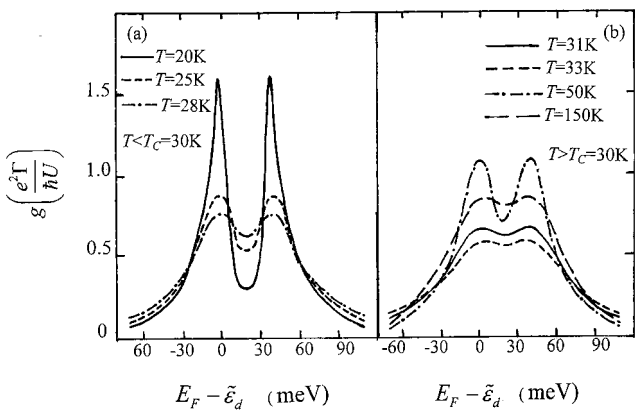

FIG. 6. Conductance, in units of $(\Gamma/U)(e^2/\hbar)$, vs energy difference between the Fermi level E_F and the dot level $\tilde{\varepsilon}_d$ (or vs gate voltage) at various temperatures (a) below and (b) above T_C when $B=0$ T. The parameters are the same as in Fig. 3.

An interesting finding is that just above T_C, there is a narrow temperature range, where the conductance minimum $g_{\min}$ at $E_F-\tilde{\varepsilon}_d=20$ meV between the two CB peaks decreases with increasing temperature. This is shown more clearly in Fig. 7, where the calculated $g_{\min}$ has been plotted against temperature for three values of U. The decrease in g with increasing T is one of the most remarkable signatures of the Kondo resonance in the quantum dots.[31–37] However, in our model for the FSQDs this anomaly, which becomes more apparent with increasing U, is not related to the higher order correlations in the leads, as in the case of the nonmagnetic QDs, since these correlations were neglected totally in the derivation of Eqs. (27) and (28). Instead, in the FSQDs the large decrease in the level broadenings with increasing T at $T>T_C$, as shown in Fig. 3, causes the anomalous T dependence of g, i.e., the CB effect becomes more prominent as the level broadenings and the overlap between the levels decrease. The external magnetic field B also causes shifts of the conductance peaks due to the giant Zeeman splitting, as shown in Fig. 8, where we now have $J_{sp\text{-}d}=0.2$ eV and $T_C=50$ K.

The most interesting finding is that the broad conductance peak at $B=0$ T and at $T\geq 30$ K is split into two peaks with increasing B. Again, this behavior is one of the specific signatures of the Kondo resonance in nonmagnetic QDs.[33] However, in the case of FSQDs, the splitting is not related to the ordinary Kondo resonance since it may occur even at Curie temperature $T_C=50$ K, as shown in Fig. 8(d), which can be much higher than the Kondo temperature T_K (in our case $T_K\ll\sqrt{\Gamma U}/2k_B\approx 27$ K with $U=40$ meV and $\Gamma=0.5$ meV). Our model for FSQDs also predicts a large magnetoresistance $(\mathrm{MR})=[g(B=0\ \mathrm{T})-g(B)]/g(B=0\ \mathrm{T})$ at low temperatures, as shown in Fig. 8. MR is largest at the two resonance peaks, and it changes sign from negative to positive at $T\leq 30$ K, when the Fermi energy E_F shifts from

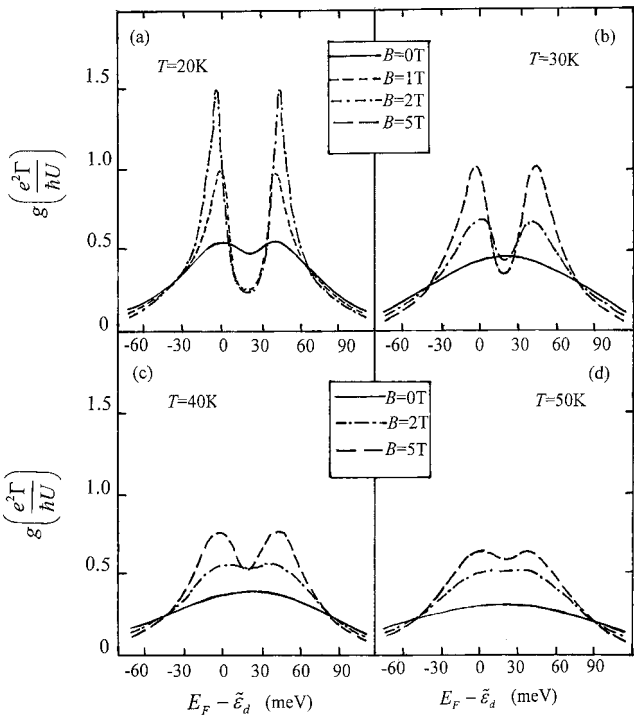

FIG. 8. Conductance, in units of $(\Gamma/U)(e^2/\hbar)$, vs energy difference between the Fermi level E_F and the dot level $\tilde{\varepsilon}_d$ (or vs gate voltage) at various temperatures and at various magnetic fields. Here we have $J_{\text{exch}}^{s\text{-}d}=0.2$ eV and $T_C=50$ K, the other parameters are the same as in Fig. 3.

$\tilde{\varepsilon}_d$ to $\tilde{\varepsilon}_d+U/2$. However, MR remains negative for all the values of E_F at higher temperatures $T>30$ K.

With the parameters used in the calculations of the results of Figs. 4–8, the Zeeman splitting $\Delta_{sp\text{-}d}^{d}$ is small even at low temperatures, which explains why there is only a minor shift of the conductance peaks at $E_F=\tilde{\varepsilon}_d$ and $E_F=\tilde{\varepsilon}_d+U$ with decreasing temperature. More prominent shifts of the peaks occur, however, if we increase the value for the exchange parameter to $J_{sp\text{-}d}=0.8$ eV (valid for holes), as shown in Fig. 9(a). Due to the very large level broadenings ($\gamma_i \approx 100$ meV at $T\approx T_C$), U must be larger than 20 meV in order for some sign of the CB effect to be found at least at low temperatures, as shown in Fig. 9(b). However, as discussed above, due to various approximations the estimated level broadenings probably are too large in our model. Therefore, we may expect that in real FSQDs, the CB effect could be seen, at least at low temperatures $T\ll T_C$ even in the case of smaller U.

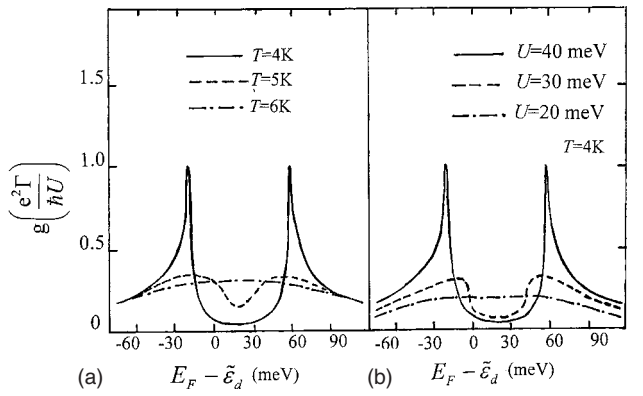

FIG. 9. Conductance, in units of $(\Gamma/U)(e^2/\hbar)$, vs energy difference between the Fermi level E_F and the dot level $\tilde{\varepsilon}_d$ (or vs gate voltage) (a) at various temperatures below $T_C=30$ K when $U=40$ meV and (b) for various values of U at $T=4$ K when $B=0$ T. The other parameters are the same as in Fig. 3.

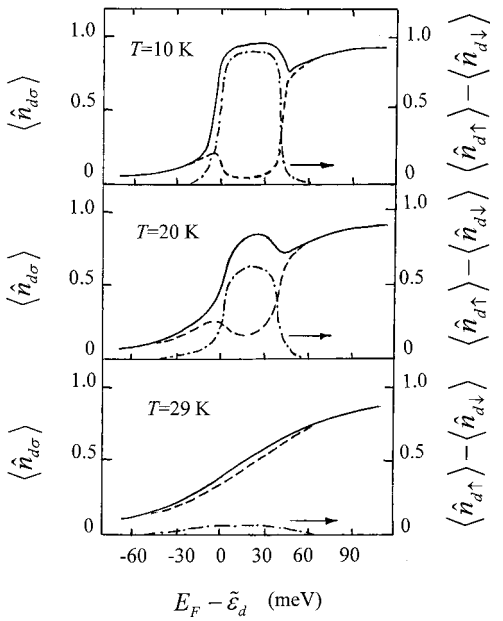

FIG. 10. Occupation probabilities $\langle\hat{n}_{d\uparrow}\rangle$ (solid curve), $\langle\hat{n}_{d\downarrow}\rangle$ (dashed curve), and the spin accumulation $\langle\hat{n}_{d\uparrow}\rangle-\langle\hat{n}_{d\downarrow}\rangle$ vs energy difference between the Fermi level E_F and the dot level $\tilde{\varepsilon}_d$ (or vs gate voltage) at various temperatures when $B=0$ T. The parameters are the same as in Fig. 3.

So far, there are no experimental results for magnetotransport in a FSQD coupled to nonmagnetic leads. Wunderlich *et al.*[30] studied experimentally the CB effect in a Mn-doped GaAs SET consisting of small islands created by potential fluctuations in the channel. However, both the leads and the islands in the SET were Mn-doped. No ferromagnetic ordering was reported, and the small amount of Mn (2%) implies a very low T_C .[20] In any case, the results indicate that magnetic, probably even ferromagnetic semiconductor SETs and quantum dots can be fabricated for transport measurements. Then the novel effects predicted by our model could be tested experimentally, e.g., by comparing the magnetotransport properties of the nonmagnetic and ferromagnetic SETs made of GaAs and Mn-doped GaAs, respectively.

E. Spin accumulation

Figure 10 shows the occupation probabilities $\langle\hat{n}_{d\sigma}\rangle$ and the spin accumulation $\langle\hat{n}_{d\uparrow}\rangle-\langle\hat{n}_{d\downarrow}\rangle$ vs gate voltage in a FSQD with the parameters of Fig. 3. At low temperatures in the CB regime $\langle\hat{n}_{d\uparrow}\rangle\gg\langle\hat{n}_{d\downarrow}\rangle$, i.e., the transport is dominated by the spin-up electrons, and there is a large spin accumulation in the energy range between $\tilde{\varepsilon}_d$ and $\tilde{\varepsilon}_d+U$. Also in this energy range the spin accumulation decreases rapidly, when the tem-

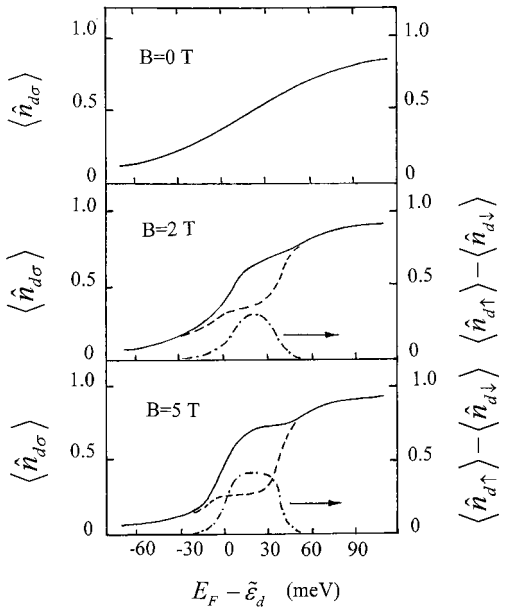

FIG. 11. Occupation probabilities $\langle \hat{n}_{d\uparrow} \rangle$ (solid curve), $\langle \hat{n}_{d\downarrow} \rangle$ (dashed curve), and the spin accumulation $\langle \hat{n}_{d\uparrow} \rangle - \langle \hat{n}_{d\downarrow} \rangle$ vs energy difference between the Fermi level E_F and the dot level $\tilde{\varepsilon}_d$ (or vs gate voltage) at various magnetic fields when $T=32$ K $> T_C = 30$ K. The parameters are the same as in Fig. 3.

perature approaches $T_C=30$ K, but the dot remains approximately singly occupied, $\langle \hat{n}_{d\uparrow} \rangle \approx \langle \hat{n}_{d\downarrow} \rangle \approx 0.5$.

Figure 11 shows the effect of an external magnetic field on the occupation probabilities at a temperature 32 K close to T_C. There is no net spin polarization of the charge carriers at zero field. However, a large spin accumulation appears with increasing magnetic field, when the system approaches the CB regime.

V. CONCLUSIONS

We have analyzed theoretically charge transport through a ferromagnetic semiconductor quantum dot in the Coulomb blockade regime. The strong *sp-d* exchange interaction between the localized magnetic moments and the charge carrier spins causes the giant Zeeman splitting of the dot energy levels, and the spin-disorder scattering of the carriers inside the dot. The scattering depends strongly on temperature and magnetic field at temperatures close to the Curie temperature, where the spin fluctuations in the ferromagnetic subsystem are largest. This results in a conductance behavior, which is similar to the Kondo resonance in nonmagnetic QDs. The predicted large spin-flip scattering means a very short spin-life time, which should be taken into account when considering the spintronic applications based on the FSQDs. The model we have treated is a simple one, and it could be improved in many ways. For instance, the spin-orbit coupling, which also causes spin-flip scattering, should be added to the present spin-disorder scattering model. Although the present formalism included the multilevel system, we neglected the transitions to the higher levels, which do not take part in charge transport. In the case of the FSQDs made from Mn-doped GaAs the real valence band structure including the light and heavy holes and the split-off band should be taken into account. The coupling due to tunneling between the dot and the current leads depends on the dot energy levels, which should be considered, especially in the case of a large Coulomb repulsion. However, in spite of all these neglected effects, we believe that our model can provide qualitatively correct predictions for FSQDs. Especially, we believe that the large level broadening and its strong temperature and magnetic field dependences are relevant in the interpretation of the results of future magnetotransport measurements in FSQDs.

ACKNOWLEDGMENTS

This work was supported by the Academy of Finland.

[1] *Semiconductor Spintronics and Quantum Computation*, edited by D. D. Awschalom, D. Loss, and N. Samarth (Springer, Berlin, 2002).
[2] I. Zutic, J. Fabian, and S. Das Sarma, Rev. Mod. Phys. **76**, 323 (2004).
[3] S. A. Wolf, D. D. Awschalom, R. A. Buhrman, J. M. Daughton, S. von Molnar, M. L. Roukes, A. Y. Chtchelkanova, and D. M. Treger, Science **294**, 1488 (2001).
[4] G. A. Prinz, Science **282**, 1660 (1998).
[5] D. P. DiVincenzo, Science **270**, 255 (1995); M. A. Nielsen and I. L. Chuang, *Quantum Computation and Quantum Information* (Cambridge University Press, Cambridge, 2000).
[6] D. Loss and D. P. DiVincenzo, Phys. Rev. A **57**, 120 (1998).
[7] H.-A. Engel and D. Loss, Science **309**, 586 (2005); J. C. Egues, *ibid.* **309**, 565 (2005).
[8] T. Hayashi, T. Fujisawa, H. D. Cheong, Y. H. Jeong, and Y. Hirayama, Phys. Rev. Lett. **91**, 226804 (2003).
[9] J. M. Elzerman, R. Hanson, L. H. Willems van Beveren, B. Witkamp, L. M. K. Vadersypen, and L. P. Kouwenhoven, Nature (London) **430**, 431 (2004).
[10] M. Kroutvar, Y. Ducommun, D. Heiss, M. Bichler, D. Schuh, G. Abstreiter, and J. J. Finley, Nature (London) **432**, 81 (2004).
[11] R. Hanson, L. H. Willems van Beveren, I. T. Vink, J. M. Elzerman, W. J. M. Naber, F. H. L. Koppens, L. P. Kouwenhoven, and L. M. K. Vandersypen, Phys. Rev. Lett. **94**, 196802 (2005).
[12] F. H. L. Koppens, C. Buizert, K. J. Tielrooij, I. T. Vink, K. C. Nowack, T. Meunier, L. P. Kouwenhoven, and L. M. K. Vandersypen, Nature (London) **442**, 766 (2006).
[13] L. P. Kouwenhoven, J. M. Elzerman, R. Hanson, L. H. Willems van Beveren, and L. M. K. Vandersypen, Phys. Status Solidi B **243**, 3682 (2006).
[14] R. M. Potok, J. A. Folk, C. M. Marcus, V. Umansky, M. Hanson,

and A. C. Gossard, Phys. Rev. Lett. **91**, 016802 (2003).
[15] D. Pfannkuche and S. E. Ulloa, Phys. Rev. Lett. **74**, 1194 (1995).
[16] D. Weinmann, W. Hausler, and B. Kramer, Phys. Rev. Lett. **74**, 984 (1995).
[17] S. Takahashi and S. Maekawa, Phys. Rev. Lett. **80**, 1758 (1998).
[18] H. Ohno, H. Munekata, T. Penney, S. von Molnar, and L. L. Chang, Phys. Rev. Lett. **68**, 2664 (1992).
[19] H. Ohno, A. Shen, F. Matsukura, A. Oiwa, H. Endo, S. Katsumoto, and Y. Iys, Appl. Phys. Lett. **69**, 363 (1996).
[20] H. Ohno and F. Matsukura, Solid State Commun. **117**, 179 (2001).
[21] L. Besombes, Y. Leger, L. Maingault, D. Ferrand, H. Mariette, and J. Cibert, Phys. Rev. Lett. **93**, 207403 (2004).
[22] T. Gurung, S. Mackowski, L. M. Smith, H. E. Jackson, W. Heiss, J. Kossut, and G. Karczewski, J. Appl. Phys. **96**, 7407 (2004).
[23] S. Lee, M. Dobrowolska, and J. K. Furdyna, Phys. Rev. B **72**, 075320 (2005).
[24] P. Wojnar, J. Suffczynski, K. Kowalik, A. Golnik, G. Karczewski, and J. Kossut, Phys. Rev. B **75**, 155301 (2007).
[25] Y. Leger, L. Besombes, J. Fernandez-Rossier, L. Maingault, and H. Mariette, Phys. Rev. Lett. **97**, 107401 (2006).
[26] R. M. Abolfath, P. Hawrylak, and I. Zutic, Phys. Rev. Lett. **98**, 207203 (2007).
[27] K. M. Hanif, R. W. Meulenberg, and G. F. Strouse, J. Am. Chem. Soc. **124**, 11495 (2002).
[28] D. A. Schwartz, N. S. Norberg, Q. P. Nguyen, J. M. Parker, and D. R. Gamelin, J. Am. Chem. Soc. **125**, 13205 (2003).
[29] M. Holub, S. Chakrabarti, S. Fathpour, P. Bhattacharya, Y. Lei, and S. Ghosh, Appl. Phys. Lett. **85**, 973 (2004).
[30] J. Wunderlich, T. Jungwirth, B. Kaestner, A. C. Irvine, A. B. Shick, N. Stone, K. Y. Wang, U. Rana, A. D. Giddings, C. T. Foxon, R. P. Campion, D. A. Williams, and B. L. Gallagher, Phys. Rev. Lett. **97**, 077201 (2006).
[31] T. K. Ng and P. A. Lee, Phys. Rev. Lett. **61**, 1768 (1988); L. I. Glazman and M. E. Raikh, JETP Lett. **47**, 452 (1988).
[32] Y. Meir, N. S. Wingreen, and P. A. Lee, Phys. Rev. Lett. **70**, 2601 (1993); N. S. Wingreen and Y. Meir, Phys. Rev. B **49**, 11040 (1994); Y. Meir, N. S. Wingreen, and P. A. Lee, Phys. Rev. Lett. **66**, 3048 (1991).
[33] T. A. Costi, Phys. Rev. B **64**, 241310(R) (2001).
[34] D. Goldhaber-Gordon, J. Göres, M. A. Kastner, H. Shtrikman, D. Mahalu, and U. Meirav, Phys. Rev. Lett. **81**, 5225 (1998).
[35] S. M. Cronenwett, T. H. Oosterkamp, and L. Kouvenhoven, Science **281**, 540 (1998).
[36] F. Simmel, R. H. Blick, J. P. Kotthaus, W. Wegscheider, and M. Bichler, Phys. Rev. Lett. **83**, 804 (1999).
[37] W. G. van der Wiel, S. De Franceschi, T. Fujisawa, J. M. Elzerman, S. Tarucha, and L. P. Kouvenhoven, Science **289**, 2105 (2000).
[38] K. Chang, K. S. Chan, and F. M. Peeters, Phys. Rev. B **71**, 155309 (2005).
[39] F. Qu and P. Vasilopoulos, Appl. Phys. Lett. **89**, 122512 (2006).
[40] J. Fernandez-Rossier and R. Aguado, Phys. Rev. Lett. **98**, 106805 (2007).
[41] S. Takahashi and S. Maekawa, Phys. Rev. Lett. **80**, 1758 (1998).
[42] X. H. Wang and A. Brataas, Phys. Rev. Lett. **83**, 5138 (1999).
[43] N. Serqueev, Q.-f. Sun, H. Guo, B. G. Wang, and J. Wang, Phys. Rev. B **65**, 165303 (2002).
[44] B. R. Bulka and S. Lipinski, Phys. Rev. B **67**, 024404 (2003).
[45] I. Weymann, J. Barnas, J. König, J. Martinek, and G. Schön, Phys. Rev. B **72**, 113301 (2005).
[46] Y. Utsumi, J. Martinek, G. Schön, H. Imamura, and S. Maekawa, Phys. Rev. B **71**, 245116 (2005).
[47] F. M. Souza, J. C. Egues, and A. P. Jauho, Phys. Rev. B **75**, 165303 (2007); K. Chang, K. S. Chan, and F. M. Peeters, *ibid.* **71**, 155309 (2005).
[48] W. Rudzinski and J. Barnas, Phys. Rev. B **64**, 085318 (2001).
[49] R. Lopez and D. Sanchez, Phys. Rev. Lett. **90**, 116602 (2003).
[50] Q. F. Sun, J. Wang, and H. Guo, Phys. Rev. B **71**, 165310 (2005).
[51] B. Dong, G. H. Ding, H. L. Cui, and X. L. Lei, Europhys. Lett. **69**, 424 (2005).
[52] W. Yang and K. Chang, Phys. Rev. B **72**, 075303 (2005).
[53] D. N. Zubarev, *Nonequilibrium Statistical Thermodynamics* (Consultant Bureau, New York, 1974).
[54] L. Jacak, P. Hawrylak, and A. Wojs, *Quantum Dots* (Springer, Berlin, 1998).
[55] P. Kuivalainen, Phys. Status Solidi B **227**, 449 (2001).
[56] C. Lacroix, J. Phys. F: Met. Phys. **11**, 2389 (1981).
[57] N. Lebedeva and P. Kuivalainen, Phys. Status Solidi B **242**, 1660 (2005).
[58] H. Haug and A.-P. Jauho, *Quantum Kinetics in Transport and Optics of Semiconductors* (Springer-Verlag, Berlin, 1998).
[59] J. Sinkkonen, Phys. Rev. B **19**, 6407 (1979).
[60] W. Heimbrodt, Th. Hartmann, P. J. Klar, M. Lampalzer, W. Stolz, K. Volz, A. Schaper, W. Treutmann, H.-A. Krug von Nidda, A. Loidl, T. Ruf, and V. F. Sapega, Physica E (Amsterdam) **10**, 175 (2001).
[61] J. Szczytko, W. Mac, A. Stachow, A. Twardowski, P. Becla, and J. Tworzydlo, Solid State Commun. **99**, 927 (1996).
[62] H. Ohno, N. Akiba, F. Matsukura, A. Shen, K. Ohtani, and Y. Ohno, Appl. Phys. Lett. **73**, 363 (1998).
[63] J. Sinkkonen, Phys. Rev. B **23**, 6638 (1981).
[64] R. M. White, *Quantum Theory of Magnetism* (McGraw-Hill, New York, 1970).
[65] M. Takahashi, K. Mitsui, and M. Umehara, Phys. Rev. B **48**, 17053 (1993).